Effects of Static and Dynamical Disturbance Forces on the Performance of a Wire Driven Flexible Robot

Mona Tahmasebi [1,*], Mohammad Gohari [2], Ali Zolfagharian [3], Mohammad Reza Zare [4], Abbas Pak [5]
[1] Agricultural Engineering Research Department, Markazi Agricultural and Natural Resources Research and Education Center, Agricultural Research, Education and Extension, Organization (AREEO), Arak, 3818385149, Iran
[2] Department of Solid Mechanics, Faculty of Mechanical Engineering, Arak University of Technology, Arak, 3818146763, Iran
[3] Faculty of Sci Eng & Built Env, Deakin University, Australia
[4] Master Student, FEMTO-ST Institute, France
[5] Department of Mechanical Engineering, Bu-Ali Sina University, Hamedan, Iran
Email: [1] Tahmasebi.mona@gmail.com, [2] moh-gohari@arakut.ac.ir
*Corresponding Author

***Abstract*—Robot requests are increased by recent development of IoT, telemetry and human requirements in uninteresting or precision jobs such as surgery, industrial inspections or crops harvesting. Numerous robots are industrialized by researchers for various tasks. Flexible robots are developed based on declared requests since they can adapt their geometry to the working circumstances. Existing study presents a wire driven flexible robot enthused of animal organs such as octopus tentacles or elephant`s trunk. It can move in planar and space based on assembly of that. Primarily, a kinematic model founded to estimate end effector location, formerly a dynamic model established to compute essential tension of tendon based on bending beam theory. Moreover, effects of static and dynamical load applied on the WDFR are studied as external disturbances. A test rig is fabricated to assess attained models. The results demonstrate close convergence between tests outcomes and outputs of models. Accordingly, dynamic and kinematic models can be operated in design of controller in coming works.**

***Keywords*—Wire Driven Robot, Flexible Robot, Kinematics and Dynamics of Robot, Trajectory of Manipulator**

I. INTRODUCTION

One of the applicable robots in various operations is wire driven flexible manipulator [1] which employed by researchers working in medical engineering field [2]-[5], fish inspired submarines [7]-[9], inspection of turbines etc. [6], harvesting and sorting of agricultural crops [10]. Most of mentioned applications, the robot arm must be compact, flexible and adaptive in geometry to have superior performance. The wire driven flexible robots (WDFR) are proper, but their ability in supporting payload and accuracy is restricted. WDFRs compared to jointed arm robots have some advantages such as few numbers of actuators, simpler in construction, and adaptation in working space conditions. During inspection operations, payload and accuracy in positioning are not imperative while in robotic surgery positioning is crucial. Moreover, external loads from environment are important in terms of manipulator arm deformation. In addition, in robotic crops harvester positioning precision is not important as much as payload capacity to grip and pick up the fruits.

Most of modeling of WDFRs is based on continues bending bar or Bernoulli-Euler beam due to bending shape generated by tendons movement [11]-[15]. Proposed models are utilized to predict WDFRs deformation of body exposed to external loads. Loading conditions are mostly simple thus they are not proper for real condition of operations [16][17]. So, kinematic and dynamic models are required to present behavior of WDFRs when subjected to complex external loading such as vibrations or base excitation. An accurate model can present positioning by acceptable precision and calculate driving force in terms of dynamic inverse to reach desired position. Such this dynamical model can be employed in design of intelligent controllers [18]-[22] although some efforts were conducted in design of controller for wire driven robots [23]-[26].

Current study aims to present a kinematic and dynamic model of WDFR in presence of static and dynamical loads as undesirable disturbances and verify accuracy of those by some experimental tests. By attained model, the curvature of arm robot can be reached, and effects of external disturbances also can be calculated.

II. METHODOLOGY

As mentioned previously, kinematic model of WDFRs is required to have suitable positioning of end effector of manipulator. Therefore, in this paper firstly kinematic model is described, then dynamic model is stated to make possible prediction of required tensions of tendons to access desired position. These parts are explained in following.

A. Kinematic Model of WDFR

The WDFR includes vertebras, tendon wires, driver motors, and base. The vertebra shape is conical, and a set of them are located together as chain. Thus, each of vertebra have three directions of rotation by spherical joint between them. The tendon wires passed of all vertebras and connected to servomotors as actuators. Fig. 1 illustrate the configuration of planar a WDFR. When one of the wires is pulled, so the

second wire is released by actuator levers. This action causes bending of WDFR. Consequently, set of vertebras is bended as cantilever beam, and total length deforms as arc of circle which has particular curvature. The radius of curvature is calculatedly based on beam bending theory. Fig. 2 shows bending of WDFR, and curvature radius is depicted on that.

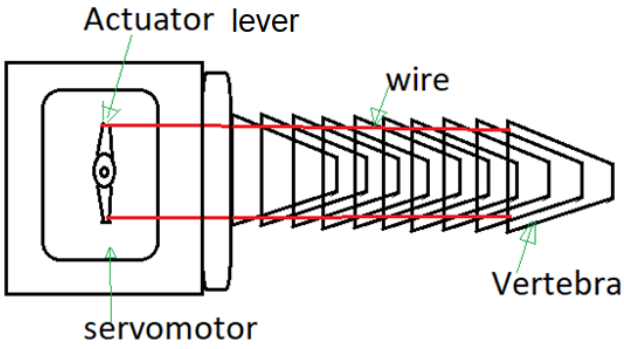

Fig. 1. WDFR parts in planar motion

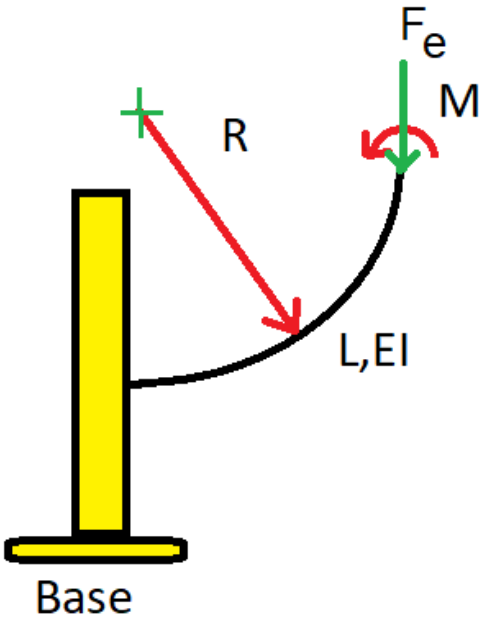

Fig. 2. Radius curvature of bended WDFR exposed to external load

The end effector of manipulator's location is presented by P(x,y), and radius of curvature is called R. As can be seen in Fig. 3, y can be obtained as:

$$y = R - R\cos\propto = R(1-\cos\propto) \tag{1}$$

On the other hand, the bending bar is arc of circle. So, x is given by:

$$x^2 + y^2 = R^2 \rightarrow x = \sqrt{R^2 - y^2} \tag{2}$$

By combining Eq. (1) and Eq. (2), consequently x is reached as function of R:

$$x = R\sqrt{2\cos\propto - \cos^2\propto}\ or\ x = Rsin\propto \tag{3}$$

The axe angle of arc is noted by α. Thus, the kinematic of WDFR is govern. Now, the curvature radius "R" is computed by bending moment as:

$$\frac{1}{R} = \frac{M}{EI} \rightarrow R = \frac{EI}{M} \tag{4}$$

Where, E is module elasticity, and I is second moment of area of beam. To calculate of M, dynamic model of WDFR must be established.

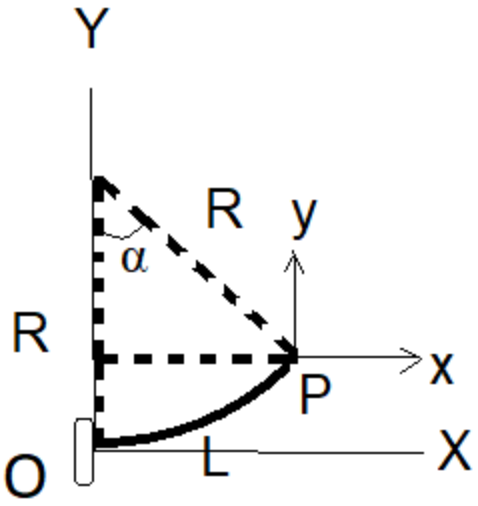

Fig. 3. Position of end effector regards to radius of curvature

B. *Dynamic Model of the WDFR*

In the bended beam, the relationship between mechanical moment and curvature radius are stated as bellow:

$$EI\frac{d^2y}{dx^2} = M \tag{5}$$

$$\frac{1}{R} = \frac{d^2y}{dx^2} \tag{6}$$

On the other hand, the created mechanical normal stress due to tension of wire is gotten by:

$$\sigma = \frac{Mc}{I} \rightarrow \tag{7}$$

The normal stress is reached by dividing tension force (F) to cross area (A):

$$\frac{F}{A} = \frac{Mc}{I} \rightarrow M = \frac{IF}{cA} \tag{8}$$

From Eq. (4) and Eq. (8), the required tension of tendon "F" to access desired curvature "R" is governed as:

$$F = \frac{AcE}{R} \tag{9}$$

Moreover, in the cantilever bar as a WDFR, the deflection of bar tip (y) or end effector when exposed to external force as disturbances, F_e, is computed by:

$$y = \frac{ML^2}{2EI} + \frac{F_eL^3}{3EI} \tag{11}$$

Hence, the dynamic model of the WDFR is acquired regards to identified position from R and M. Now, both of position of end effector and required tension of wire are available, then design of controller of the WDFR is possible.

(a)

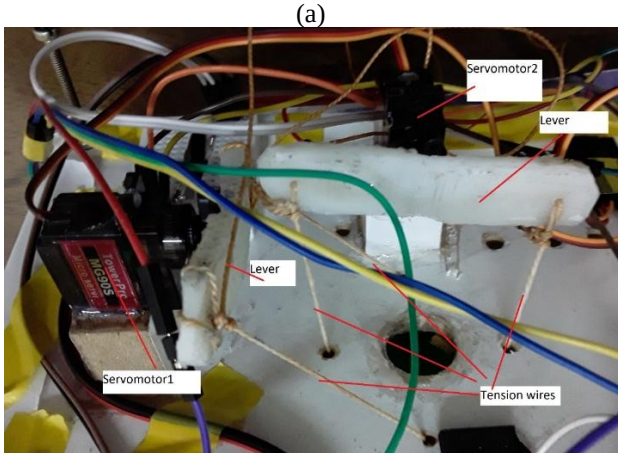

(b)

Fig. 4. The developed WDFR

Also, by the achieved kinematic and dynamic models of the WDFR, a computer program is provided to calculate end effector position based on wires tensions. The computed position of end effector regards to wire tension changes is illustrated in Fig. 5. As can be seen, the high of end effector is raised by increasing the wire tension. In this case, the module of elasticity is 100kPa.

C. Conducted Experiments of the WDFR

To evaluate the accuracy of dynamic and kinematic model of the WDFR, a robotic arm is developed which can work in 2D work space (planar) and 3D. Ten vertebras by 45mm length and 15mm radius are connected by 4 wires. End of each pair of wires fasted to the servomotors lever. By this configuration, rotation of lever of servomotor leads to impose the tension of wires. The experimental set up is revealed in Fig. 4(a). Control of servomotors is applied by an Arduino UNO board. The tension of wires is measured by spring dynamometer as 0.25 N in each 45 degree of motor rotation. The location of mounted servomotors is considered behind plate base of robot as depicted in Fig. 4(b). The position of end effector is measured by two rulers in vertically and horizontally length.

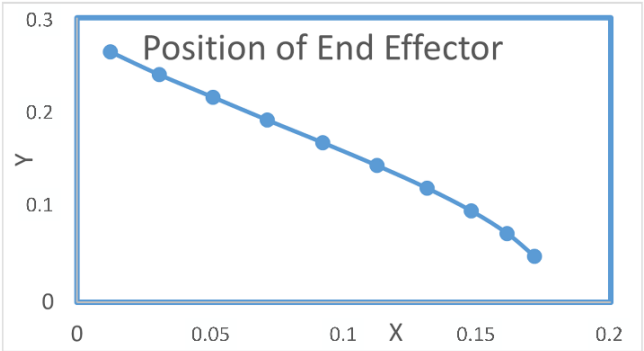

Fig. 5. Position of the end effector without disturbances

To have better sense of that, the value of X and Y are plotted vs tension force in Fig. 6 and Fig. 7, respectively. In fact, the value of X is decreased by wire tension while value of Y increased by that. The radius of curvature is diminished by force increasing as shown in Fig. 8.

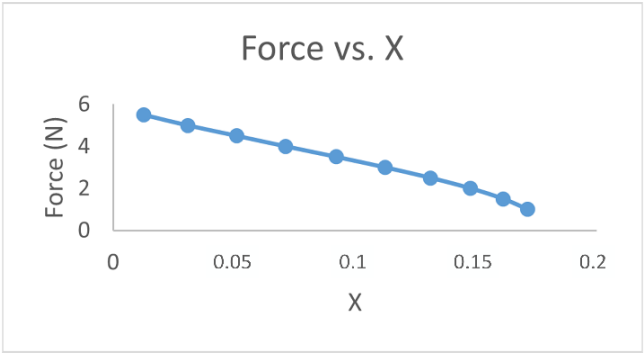

Fig. 6. The effect of tension force increasing on X

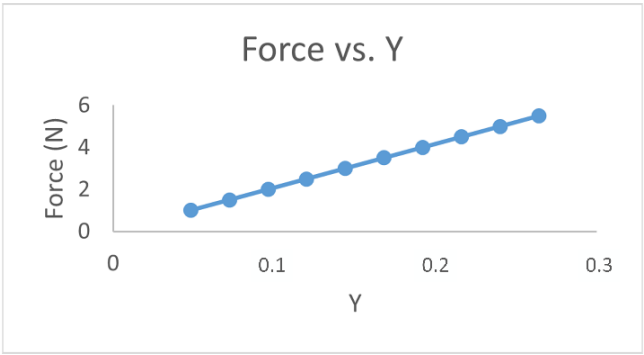

Fig. 7. The effect of tension force increasing on Y

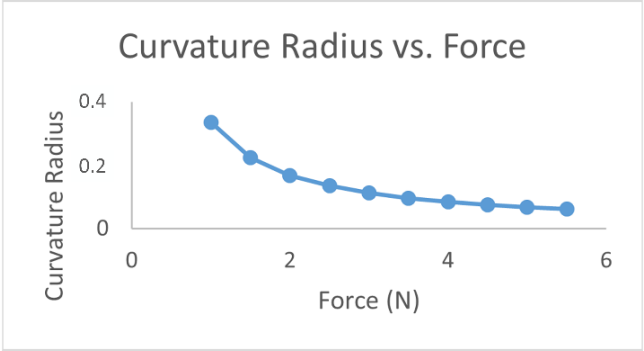

Fig. 8. Changes of curvature radius by tendon force increasing

In another case, same as previous by considering module of elasticity as 100kPa, the position of end effector is reformed as Fig. 9 when constant external load applied to the end effector. The magnitude of external load increased incrementally from 0.1N to 1N. Moreover, X is decreased while Y is increased correspondingly by the force (Fig.10 and Fig. 11). Same as last case, the curvature radius is decreased by raising of the tension force value and external load applied. It is revealed in Fig. 12.

To study effect of vibrational force on the WDFR, a seismic load with 0.05N magnitude is applied on the dynamic model of WDFR. It provides possibility to observe changes of trajectory of WDFR when this vibrational load imposing external disturbances. Thus, by occurring this dynamical load as expected, position of the end effector is influenced and shown in Fig. 13. The accuracy of positioning is decreased drastically. This variation revealed on the values of X and Y (Fig. 14 and Fig. 15). The curvature radius also changes by imposing this disturbance. Fig. 16 illustrates this variation.

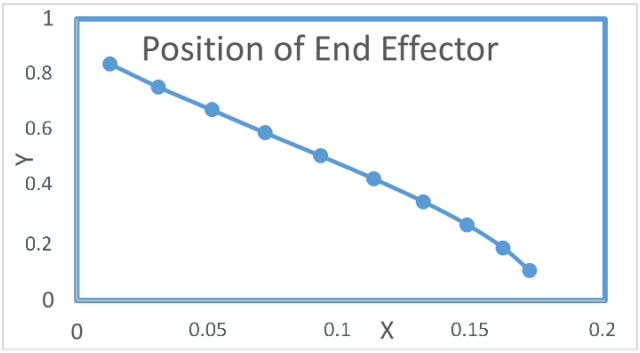

Fig. 9. The end effector position of WDFR exposed to external load

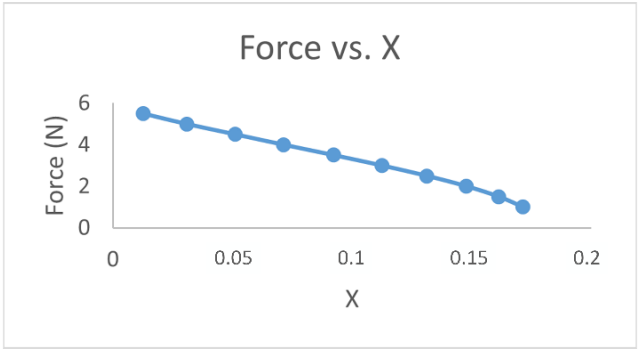

Fig. 10. X value of end effector vs. tension of wire when applied to the external load

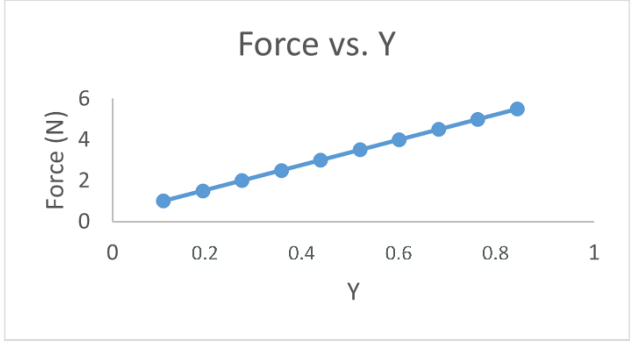

Fig. 11. Y value of end effector vs tension of wire when applied to the external load

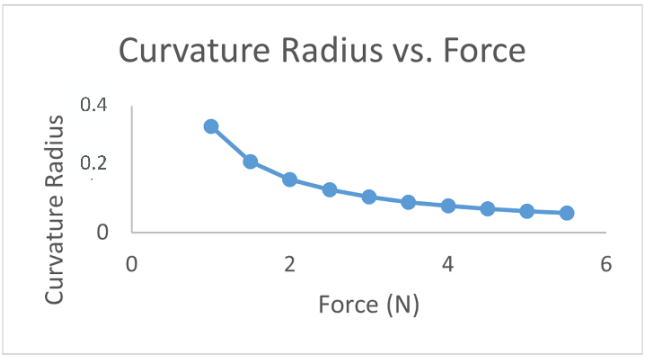

Fig. 12. Changes of curvature radius by tendon force increasing during external load applied

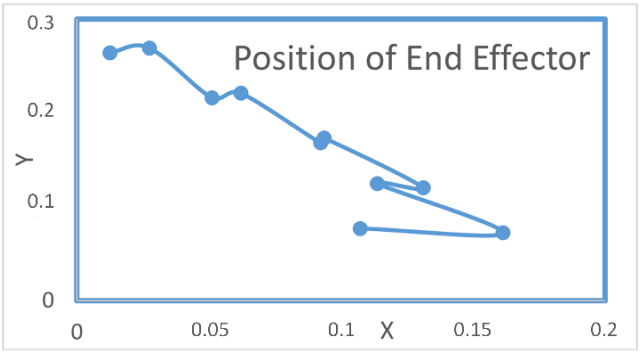

Fig. 13. Effect of vibrational load on the WDFR positioning

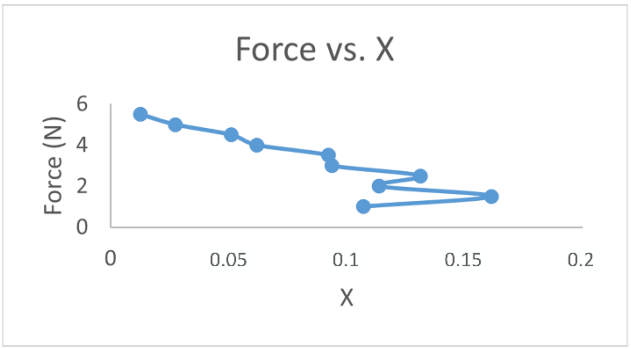

Fig. 14. Tension force of tendon vs. X when vibrational load applied

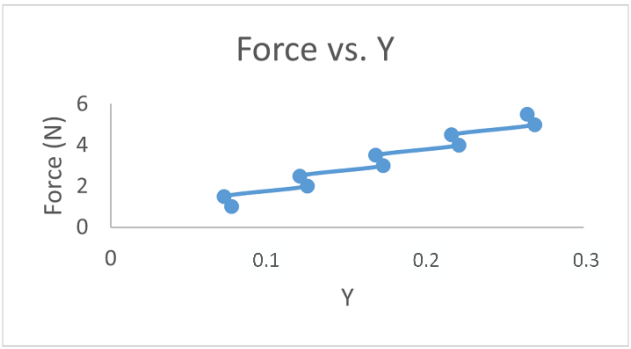

Fig. 15. Tension force of tendon vs. Y when the WDFR exposed to vibrational load

A set of experimental tests of WDFR are conducted. Various tensions of pair of wires are applied by two servomotors. By 90 degrees of rotation of servomotor lever, 0.5 N tensile force is imposed to wires. So, by 180 degree rotation of lever tensile force of tendon raises to 1N. Whereas two servomotors are installed to the WDFR base, work space is 3D. Different positions are accessed by combination of

rotating degree of two motors. In the results part, the points which are touched by different tension of two pairs of wires are shown and discussed.

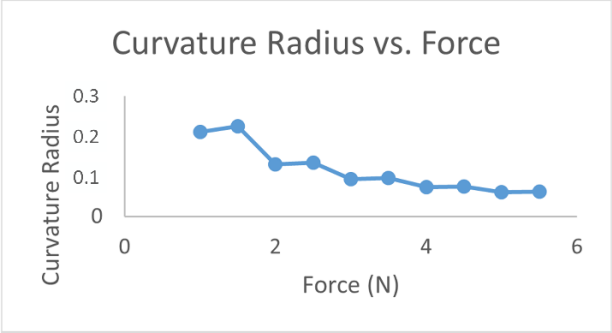

Fig. 16. Variations of curvature radius when vibrational load imposed to the WDFR

III. Results and Discussions

Different positions in work space are reached by various applied tension of tendon wires by two servomotors. To have better comparison by theoretical model, just planar motions generated by one servomotor are considered. In addition, a vibrational load exposed by minatory shaker on the WDFR. As illustrated in Fig. 17, the position of end effector is changed by produced bending due to wire tensions same as dynamical model. Although the trend of them is similar, in lower height of end effector there is differences. It seems that lower tension of wires is reason of that. In fact, by increasing tendon tension, WDFR affected less by vibrational loading. These variations can be seen in the X and Y graph when the applied force is changed (Fig.18 and Fig. 19).

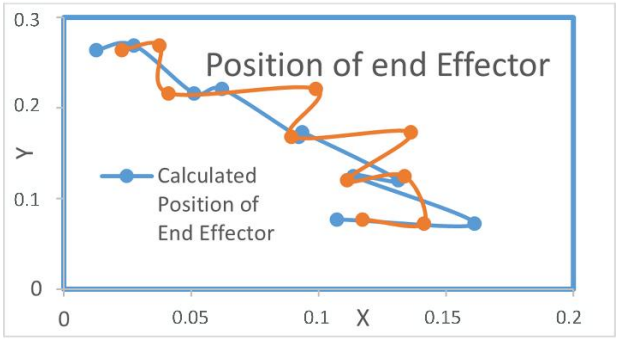

Fig. 17. Comparison of reached end effector position by theory results

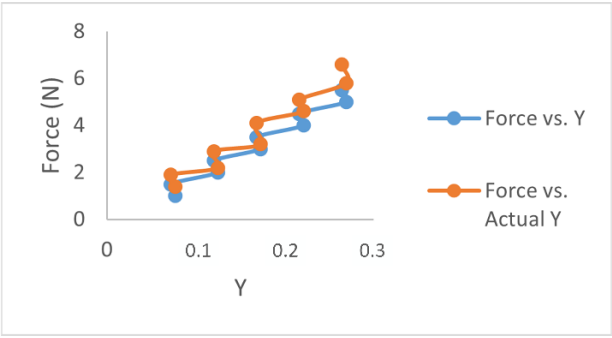

Fig. 18. The effect of force increasing on actual Y compared by theory values

The behavior of robot arm also evaluated by study of length between reference point (o) to end effector (P). It called $\bar{L}$, and it computed by:

$$\bar{L} = \sqrt{x^2 + y^2} \tag{12}$$

The actual $\bar{L}$ is plotted versus to calculated $\bar{L}$ from theoretical values in Fig. 20. The correlation ratio is reached as 0.92, and it shows closeness between experiment results and dynamical model.

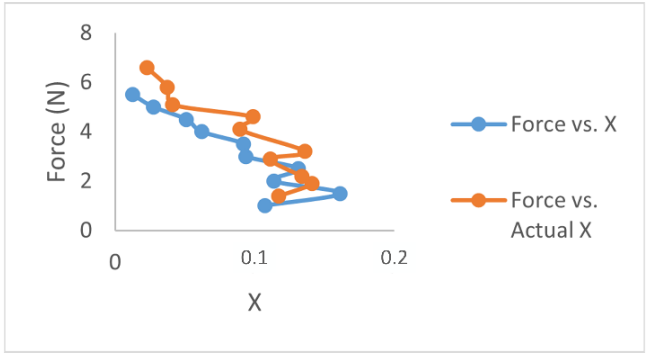

Fig. 19. The effect of force increasing on actual X compared by theory values

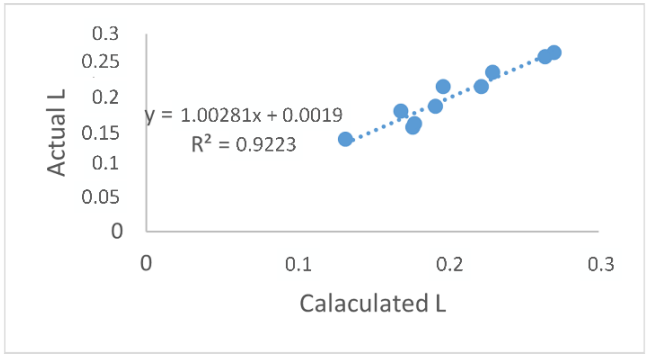

Fig. 20. The relationship between experimental $\bar{L}$ and calculated $\bar{L}$ by dynamic model

IV. Conclusion

Kinematic and dynamic models of a WDFR are govern based on beam theory when beam exposed to the statically load. The results of kinematic and dynamic model of WDFR show that accuracy and linearity of end effector position is affected by vibrational load applying on the WDFR drastically. In addition, the test results reveal convergence of outputs of model and conducted experiments such as position and applied tension of wires. This dynamic and kinematic model leads to design proper control system for various robot applications particularly vibrating disturbances occur on the manipulator body.

References

[1] K. Suzumori, S. Iikura and H. Tanaka, "Applying a flexible microactuator to robotic mechanisms," *IEEE Control Systems Magazine*, vol. 12, no. 1, pp. 21-27, 1992, https://doi.org/10.1109/37.120448.

[2] T. Fisher *et al*., "Intraoperative magnetic resonance imaging–conditional robotic devices for therapy and diagnosis," *Proceedings of the Institution of Mechanical Engineers, Part H: Journal of Engineering in Medicine*, vol. 228, no. 3, pp. 303-318, 2014, https://doi.org/10.1177/0954411914524189.

[3] H. Alfalahi, F. Renda and C. Stefanini, "Concentric Tube Robots for Minimally Invasive Surgery: Current Applications and Future Opportunities," *IEEE Transactions on Medical Robotics and Bionics*,

vol. 2, no. 3, pp. 410-424, 2020, https://doi.org/10.1109/TMRB.2020.3000899.

[4] P. E. Dupont, J. Lock, B. Itkowitz and E. Butler, "Design and Control of Concentric-Tube Robots," *IEEE Transactions on Robotics*, vol. 26, no. 2, pp. 209-225, 2010, https://doi.org/10.1109/TRO.2009.2035740.

[5] Y. Zhou, H. Ren, M. Q. H. Meng, Z. I. O. N. Tsz Ho Tse, and H. Yu, "Robotics in natural orifice transluminal endoscopic surgery," *Journal of Mechanics in Medicine and Biology*, vol. 13, no. 02, p. 1350044, 2013, https://doi.org/10.1142/S0219519413500449.

[6] Z. Li and R. Du, "Design and analysis of a biomimetic wire-driven flapping propeller," *2012 4th IEEE RAS & EMBS International Conference on Biomedical Robotics and Biomechatronics (BioRob)*, pp. 276-281, 2012, https://doi.org/10.1109/BioRob.2012.6290774.

[7] Z. Li, W. Gao, R. Du, and B. Liao, "Design and analysis of a wire-driven robot tadpole," *ASME International Mechanical Engineering Congress and Exposition*, vol. 45202, pp. 297-303, 2012, https://doi.org/10.1115/IMECE2012-87462.

[8] B. Liao, Z. Li and R. Du, "Robot tadpole with a novel biomimetic wire-driven propulsor," *2012 IEEE International Conference on Robotics and Biomimetics (ROBIO)*, pp. 557-562, 2012, https://doi.org/10.1109/ROBIO.2012.6491025.

[9] G. Chowdhary, M. Gazzola, G. Krishnan, C. Soman, and S. Lovell, "Soft robotics as an enabling technology for agroforestry practice and research," *Sustainability*, vol. 11, no. 23, p. 6751, 2019, https://doi.org/10.3390/su11236751.

[10] B. A. Jones, R. L. Gray and K. Turlapati, "Three dimensional statics for continuum robotics," *2009 IEEE/RSJ International Conference on Intelligent Robots and Systems*, pp. 2659-2664, 2009, https://doi.org/10.1109/IROS.2009.5354199.

[11] D. C. Rucker, B. A. Jones and R. J. Webster, "A model for concentric tube continuum robots under applied wrenches," *2010 IEEE International Conference on Robotics and Automation*, pp. 1047-1052, 2010, https://doi.org/10.1109/ROBOT.2010.5509701.

[12] D. B. Camarillo, C. F. Milne, C. R. Carlson, M. R. Zinn and J. K. Salisbury, "Mechanics Modeling of Tendon-Driven Continuum Manipulators," *IEEE Transactions on Robotics*, vol. 24, no. 6, pp. 1262-1273, 2008, https://doi.org/10.1109/TRO.2008.2002311.

[13] J. Lock, G. Laing, M. Mahvash and P. E. Dupont, "Quasistatic modeling of concentric tube robots with external loads," *2010 IEEE/RSJ International Conference on Intelligent Robots and Systems*, pp. 2325-2332, 2010, https://doi.org/10.1109/IROS.2010.5651240.

[14] D. C. Rucker and R. J. Webster III, "Statics and Dynamics of Continuum Robots With General Tendon Routing and External Loading," *IEEE Transactions on Robotics*, vol. 27, no. 6, pp. 1033-1044, 2011, https://doi.org/10.1109/TRO.2011.2160469.

[15] Y. Gao, K. Takagi, T. Kato, N. Shono and N. Hata, "Continuum Robot With Follow-the-Leader Motion for Endoscopic Third Ventriculostomy and Tumor Biopsy," *IEEE Transactions on Biomedical Engineering*, vol. 67, no. 2, pp. 379-390, 2020, https://doi.org/10.1109/TBME.2019.2913752.

[16] R. J. Webster III and B. A. Jones, "Design and kinematic modeling of constant curvature continuum robots: A review," *The International Journal of Robotics Research*, vol. 29, no. 13, pp. 1661-1683, 2010, https://doi.org/10.1177/0278364910368147.

[17] M. Gohari, R. A. Rahman, R. Ishak Raja and M. Tahmasebi, "Bus seat suspension modification for pregnant women," *2012 International Conference on Biomedical Engineering (ICoBE)*, pp. 404-407, 2012, https://doi.org/10.1109/ICoBE.2012.6179047.

[18] M. Gohari, R. A. Rahman, and M. Tahmasebi, "Prediction head acceleration from hand and seat vibration via artificial neural network model," *Applied Mechanics and Materials*, vol. 471, pp. 161-166, 2014, https://doi.org/10.4028/www.scientific.net/AMM.471.161.

[19] M. Gohari, M. Tahmasebi and A. Nozari, "Application of machine learning for NonHolonomic mobile robot trajectory controlling," *2014 4th International Conference on Computer and Knowledge Engineering (ICCKE)*, pp. 42-46, 2014, https://doi.org/10.1109/ICCKE.2014.6993354.

[20] M. Tahmasebi, M. Gohari, and A. Emami, "An autonomous pesticide sprayer robot with a color-based vision system," *International Journal of Robotics and Control Systems*, vol. 2, no. 1, pp. 115-123, 2022, https://doi.org/10.31763/ijrcs.v2i1.480.

[21] M. Tahmasebi, M. Mailah, M. Gohari, and R. Abd Rahman, "Vibraion suppression of sprayer boom structure using active torque control and iterative learning. Part I: Modelling and control via simulation," *Journal of Vibration and Control*, vol. 24, no. 20, pp. 4689-4699, 2018, https://doi.org/10.1177/1077546317733164.

[22] Z. Li, H. Ren, P. W. Y. Chiu, R. Du, and H. Yu, "A novel constrained wire-driven flexible mechanism and its kinematic analysis," *Mechanism and Machine Theory*, vol. 95, pp. 59-75, 2016, https://doi.org/10.1016/j.mechmachtheory.2015.08.019.

[23] Y. Niu, Y*et al*., "Control and dynamic simulation of wire-driven precise spray robotic arm," *Journal of Physics: Conference Series*, vol. 2302, no. 1, p. 012012, 2022, https://doi.org/10.1088/1742-6596/2302/1/012012.

[24] K. Misu, M. Ikeda, K. Or, M. Ando, M. Gunji, H. Mochiyama, and R. Niiyama, "Robostrich arm: Wire-driven high-dof underactuated manipulator," *Journal of Robotics and Mechatronics*, vol. 34, no. 2, pp. 328-338, 2022, https://doi.org/10.20965/jrm.2022.p0328.

[25] W. Yuqi, C. Jinjiang, G. Ranran, Z. Lei, and W. Lei, "Study on the design and control method of a wire-driven waist rehabilitation training parallel robot," *Robotica*, vol. 40, no. 10, pp. 3499-3513, 2022, https://doi.org/10.1017/S0263574722000376.

[26] K. Yoon, S. M. Cho, and K. G. Kim, "Coupling effect suppressed compact surgical robot with 7-Axis multi-joint using wire-driven method," *Mathematics*, vol. 10, no. 10, p. 1698, 2022, https://doi.org/10.3390/math10101698.